

# SYNERGISTIC INFLUENCE OF GRAPHITE ON BIOPOLYMER COMPOSITES PROPERTIES

Nur Munirah Abdullah<sup>a</sup>, Anika Zafiah M. Rus<sup>a\*</sup>, M.F.L Abdullah<sup>b</sup>

<sup>a</sup>Sustainable Polymer Engineering, Advanced Manufacturing and Material Center (AMMC), Faculty of Mechanical and Manufacturing Engineering, Universiti Tun Hussein Onn Malaysia, 86400 Parit Raja, Batu Pahat, Johor, Malaysia

<sup>b</sup>Department of Communication Engineering, Faculty of Electrical and Electronic Engineering, Universiti Tun Hussein Onn Malaysia, 86400 Parit Raja, Batu Pahat, Johor, Malaysia

## Article history

Received

15 July 2015

Received in revised form

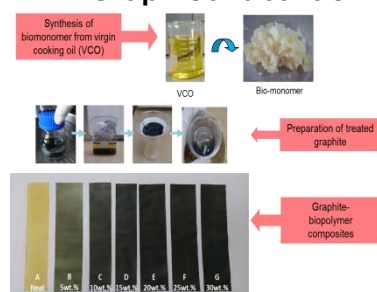
1 October 2015

Accepted

25 October 2015

\*responding author  
zafiah@uthm.edu.my

## Graphical abstract



## Abstract

Biopolymer and its cross-linker (Methylene Diphenyl Diisocyanate, MDI) were blended by weight 2:1. This is mixed with different percentages of pretreated graphite. The mixture was prepared by slip casting as thin films, at thickness of ~0.1 mm. The interface-morphology-structure relations of graphite/ biopolymer composites was diagnosed by X-Ray Diffractometer (XRD), Field Emission Scanning Electron Microscopy (FE-SEM), Fourier transform infra-red spectroscopy (FTIR) and Ultraviolet-visible (UV-vis) spectrophotometer. The homogeneously dispersed and strong interface between the graphite with/ within the biopolymer matrix influenced the current-voltage (I-V) characteristics of the thin films where the percolation threshold occurs at higher graphite loading (20 wt.%, 25 wt.% and 30 wt.%) gives conductivity of  $10^3 - 10^4$  S/m. Remarkably, graphite/ biopolymer composites makes it possible to prepare better mechanical behavior with stiff, strong yet tough properties compared with those of its neat counterpart.

**Keywords:** Graphite/ biopolymer composites, interface-morphology-structure, conductivity, mechanical behavior

## Abstrak

Biopolimer dan silang penghubungnya (Methylene Diphenyl diisocyanat, MDI) diadun mengikut nisbah berat 2: 1. Ianya dicampur bersama grafit yang dirawat mengikut peratusan yang berbeza. Campuran ini disediakan melalui slip penuangan sebagai filem nipis, pada ketebalan ~ 0.1 mm. Perkaitan hubungkait-morfologi-struktur komposit grafit / biopolimer disahkan oleh X-Ray Diffractometer (XRD), Field Emission Scanning Electron Microscopy (FE-SEM), Fourier transform infra-red spektrometer (FTIR) dan Ultraviolet-visible (UV-vis) spektrofotometer. Sebaran sebatian dan hubungkait yang antara grafit dengan / dalam matrik biopolimer mempengaruhi ciri-ciri voltan semasa (IV) filem nipis di mana ambang serapan berlaku pada penambahan grafit yang lebih tinggi (20 wt.%, 25 wt.% Dan 30 wt. %) dengan kekonduksian  $10^3-10^4$  S / m. Istimewanya, komposit grafit / biopolymer berkemungkinan untuk mempunyai sifat mekanikal yang lebih baik dengan kekakuan, kuat serta kukuh berbanding sifat asalnya.

**Kata kunci:** Grafit/ biopolimer komposit, hubungkait-morfologi-struktur, kekonduksian, sifat mekanikal

© 2015 Penerbit UTM Press. All rights reserved

## 1.0 INTRODUCTION

The emerging class of “green” electronics promise of organic electronics that is to deliver low-cost, energy efficient materials and devices, also heading unimaginable functionalities for electrical and electronics technology. By shifting the focus of electronics fabrication from the traditionally rigid glass substrates to flexible, even stretchable foil, nanocomposites (consist of functional fillers based polymer) have widely been investigated for developing high-performance materials.

The assembly of functional fillers and biopolymer properties meets many possible needs of reducing greenhouse emissions, enhancing waste management, and improving sustainability instead of reducing production cost. A catalytic ring-opening polymerization of the epoxides to form polyols (bi-monomer) is currently receiving considerable attention in a way of being biodegradable, produced from renewable resources and comprehensive study for foams [1], thin film [2], coating [3] etc. However, polymeric materials either organic or inorganic are generally electrical insulators in their nature, which greatly limits its usage as a smart material under electrical conducting application. Conductive biopolymers have many advantages over metallic conductors. They can be easily modified with low cost technologies; light weight; provide corrosion resistance and offer a wide range of electrical conductivities. In recent years, there is an increased interest in conductive polymer composites (CPC) using conductive fillers such as carbon black (CB) [4], carbon nanotubes [5-7], graphene [8] as well as graphite [9-11], as reinforcements for bio-polymeric materials due to their smart properties. Conductive polymeric composites can be used in place of metals when properties such as lightweight, easy to be tailored and corrosion resistance are required. Graphite, which is naturally abundant, is well known as traditional carbon-based filler and is recognized as the best conductive filler for its excellent conductive properties and well dispersion in polymer matrix. As previous researcher, Shih found that graphite mixed with polydimethylsiloxane (PDMS) have the highest temperature sensitivity and higher stability compared with the composites using other carbon fillers as sensor [9]. Graphite/ epoxy composites also widely used as memory and energy storage [10], plastic chip electrode [11], electromagnetic interference shielding etc. Then, a series of conducting polyaniline/expanded graphite (PA/EG) composite was synthesized by in situ polymerization of aniline in acid medium followed by the addition of expanded graphite in various proportions (1, 2 and 3 wt%). The dc electrical conductivities of the composites were dramatically increased compared with pure

polyaniline and found to be  $0.50 \times 10^2$  S/cm to  $6.11 \times 10^2$  S/cm [16].

Graphite reinforced polymeric composites have exceptional mechanical behavior which are unequalled by other materials. The material is strong, stiff, and lightweight. In recent years, Cai et al., (2013) found that with the incorporation of 4.4 wt% of graphite oxide nanoplatelets (GONPs), the Young's modulus and hardness of the polyurethane (PU) are significantly increased by ~900% and ~327%, respectively. Yasmin (2005) state that, an improvement of elastic modulus in expendable/ epoxy nanocomposite over pure epoxy can be attributed to the in situ formation of graphite nanosheets as well as uniform dispersion and exfoliation of graphite nanosheets in the former case. In this work, the graphite flakes were pretreated first via acid treatment and sonication. Then, the pretreated graphite was grafted into the biopolymer by varying the graphite weight loading (wt.%). The interface-morphology-structure relations of these free-standing composite films are explored to provide better understanding of the dispersion and particle bonding of graphite with/ within the biopolymer matrix influenced the electrical conduction dependencies. In addition, the mechanical properties of the composites are discussed.

## 2.0 EXPERIMENTAL

### 2.1 Materials

The graphite flakes used are supplied by May & Baker Ltd., Dagenham, England were used for the preparation of CPCs. The used of virgin cooking oil (VCO) as biomonomer preparation, whilst all other chemicals and reagents for the acid-catalyst preparation are of SYSTEM ChemAR. The Methylene Diphenyl Diisocyanate (MDI) from ALDRICH was used as biomonomer cross-linker.

Herein, the fabrications of graphite/ biopolymer composites are divided into steps.

### 2.2 Graphite Preparation

Flake graphite mixture and ultrasonic solvent were placed into a flask in the ultrasonic cleaning bath at room temperature. After sonication, the pretreated graphite is washed to neutrality with water, dehydrated, and dried in an oven below 60 °C for 60 min. This method has been adopted from Jihui Li in 2007 [12].

### 2.3 Biomonomer Synthesis

Biomonomer is prepared from renewable resources of virgin cooking oil (VCO). VCO is obtained and chemically manipulated at laboratory scale using less than 1L tan of VCO [13].

The biomonomer conversion begins with the catalyst preparation to generate the monomer from the unsaturated fatty compound, and second reaction is the acid-catalyst ring opening of the epoxies to form polyols or bioepoxy [14]. The mixture will be heated at 70° C and stirred for 6 hours. This will yields the biomonomer.

## 2.4 Composites Preparation

Thin films composites are prepared by mixing the biomonomer with its cross-linker, Methylene Diphenyl Diisocyanate (MDI) and pretreated graphite (with tabulated ratio as in Table 1, weighth loading 5 wt%, 10 wt, 15 wt%, 20 wt%, 25 wt%, 30 wt%) using mechanical stirrer and cast into square container which are then dried at ambient temperature for at least 6 hours. The resulting substrate films were peeled off and identified as simplified in Figure 1. Micrometer and FE-SEM images are used to measure the thickness of the sample at particular point ranging ~0.1 mm.

method with gold coating via a Keithley (USA) 6487 electrometer and then converted into electrical conductivity  $\sigma$  (S/m) with Equation (1):

**Table 1** Sample preparation with different weight percentage (wt.%) of graphite loading

Sample	Components	Weight ratio
A	Monomer/ MDI/ Graphite	2/1/0
B	Monomer/ MDI/ Graphite	2/1/0.1
C	Monomer/ MDI/ Graphite	2/1/0.2
D	Monomer/ MDI/ Graphite	2/1/0.3
E	Monomer/ MDI/ Graphite	2/1/0.4
F	Monomer/ MDI/ Graphite	2/1/0.5
G	Monomer/ MDI/ Graphite	2/1/0.6

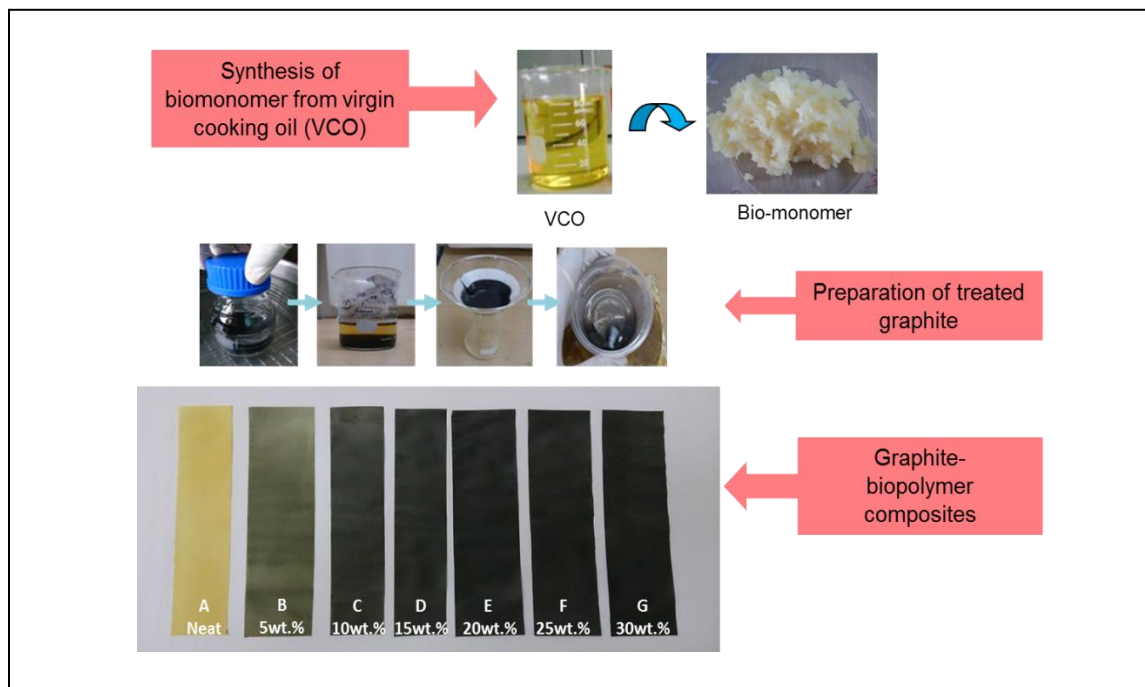


**Figure 1** Preparation of graphite/ biopolymer composites.

## 2.5 Electrical Measurement

The first characterization is the electrical conductivity of the graphite/ biopolymer composites and their reliance. The volume resistivity of the prepared samples  $\rho$  ( $\Omega$ ) was determined by a two point probe

## 2.6 The Interface-Morphology-Structure Relations

The morphology of the graphite/ biopolymer are observed using Field Emission Scanning Electron

$$\sigma = \frac{1}{\rho} + \frac{L}{RS} \quad \text{Equation (1)}$$

Where,

L (m) is the distance between clumps

R ( $\Omega$ ) is the electrical resistance

S ( $m^2$ ) is the cross sectional area

Microscopy (FE-SEM, A JEOL JSM-7600F microscope). All surfaces were sputter coated with gold to reduce the incident of surface charging in the scanning electron microscope.

X-Ray Diffractometer (XRD) Bruker D8 Advance with Cu K $\alpha$  radiation ( $\lambda = 1.541 \text{ \AA}$ ) was used within the range of  $2\theta = 10^\circ - 30^\circ$  in order to observe the crystallographic properties influenced of graphite filler in biopolymer matrix.

Meanwhile, the functional groups of the composites were identified by using PerkinElmer Fourier Transform Infrared Spectroscopy (FTIR) in the range of  $400 - 4000 \text{ cm}^{-1}$  with the resolution of  $4 \text{ cm}^{-1}$ .

Ultra-Violet visible spectrophotometry was used to record the absorb light in the UV or visible regions of the electromagnetic spectrum for the dispersions of each composite.

## 2.7 The Mechanical Behavior

According to ASTM D883 specifications, thin film specimens were cut out from graphite/ biopolymer sheets and the modulus, tensile strength, and percentage elongation at break were determined using Universal Tensile Machine (AG-I, Shimadzu, 10kN type) in which adopted from Vadukumpully [15] and Moazzami Gudarzi [16]. Noted, the cross-head speed runs at  $500 \text{ mm/min}$  at room temperature.

## 3.0 RESULTS AND DISCUSSION

### 3.1 X-Ray Study

The biopolymer formed here is a thermoset type with two different types of chain segments, hard and soft, where each has different properties. The XRD analysis in Figure 2 verifies scattered intensity distribution broad such peak ( $2\theta = 17 - 25^\circ$ ) in composites suggesting the semi crystalline structure due to the soft segments of the biopolymer. The soft segments (SS) have rubber-like properties while the hard segments tend to form crystallites which act as physical cross-links and the formation of graphite with/ within biopolymer matrix as shown in Figure 3.

The diffractions also shows the intense peak at  $2\theta$  value of  $\sim 26.4^\circ$  presence in all composites (B 5wt.% - G 30wt.% ) assigned to single graphite layers at a distance of  $0.341 \text{ nm}$ , in which similar to earlier studies

[17]. As we can see, the reduction in intensity of these peaks as graphite weight loading is increased. These pattern suggesting that the presence of graphite somehow impedes the formation of soft segment crystallites. Hence, contributes to higher crystallization properties of the biopolymer thin film composites as compared to its neat counterpart.

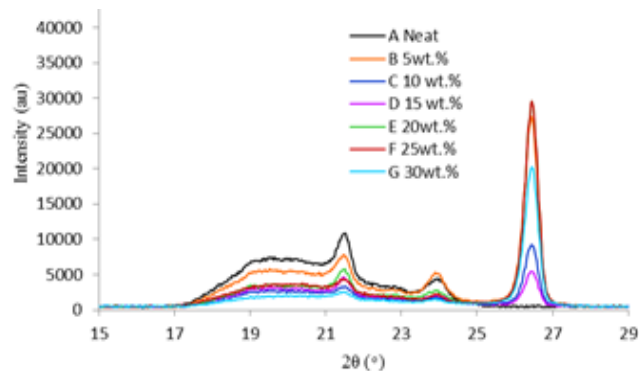


Figure 2 XRD traces of graphite/ biopolymer composites

### 3.2 Film Morphology

In previous result, it is shown that insertion of graphite into biopolymer improved crystallinity to the composites. Herein, the morphology of graphite/ biopolymer composites appear promising as determined from FE-SEM images in Figure 4. The FE-SEM images appears a typical disorder structures of pretreated graphite where randomly and homogeneously dispersed in biopolymer matrix. The pretreated graphite is not a single graphite but rather consists of several layers or aggregation of graphite sheets. It is noted that the pretreated graphite contain functional groups such as  $-\text{OH}$ ,  $-\text{COOH}$  after acid treatment which implies a strong interconnected interface between the biopolymer and pretreated graphite. Hence, promote both physical and mechanical properties and it also enhanced the electron mobilized through the polymeric matrix composites in order to achieved the percolation threshold.

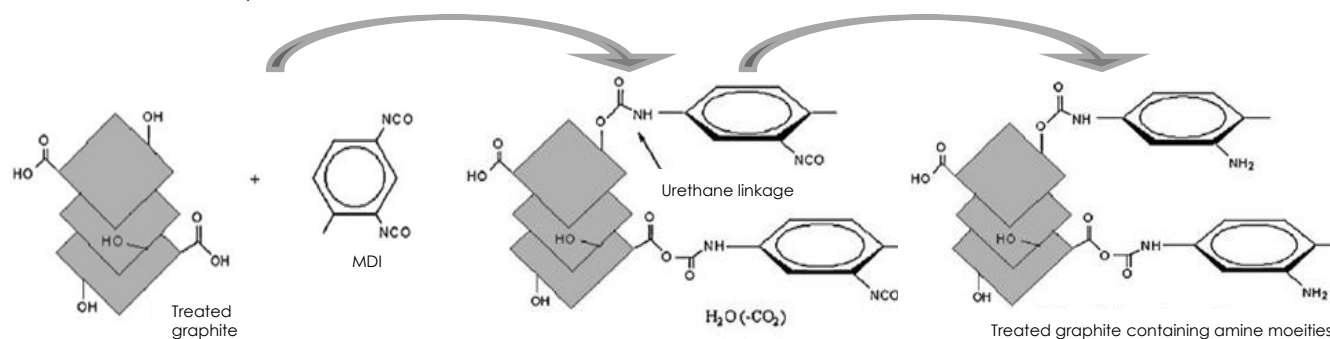
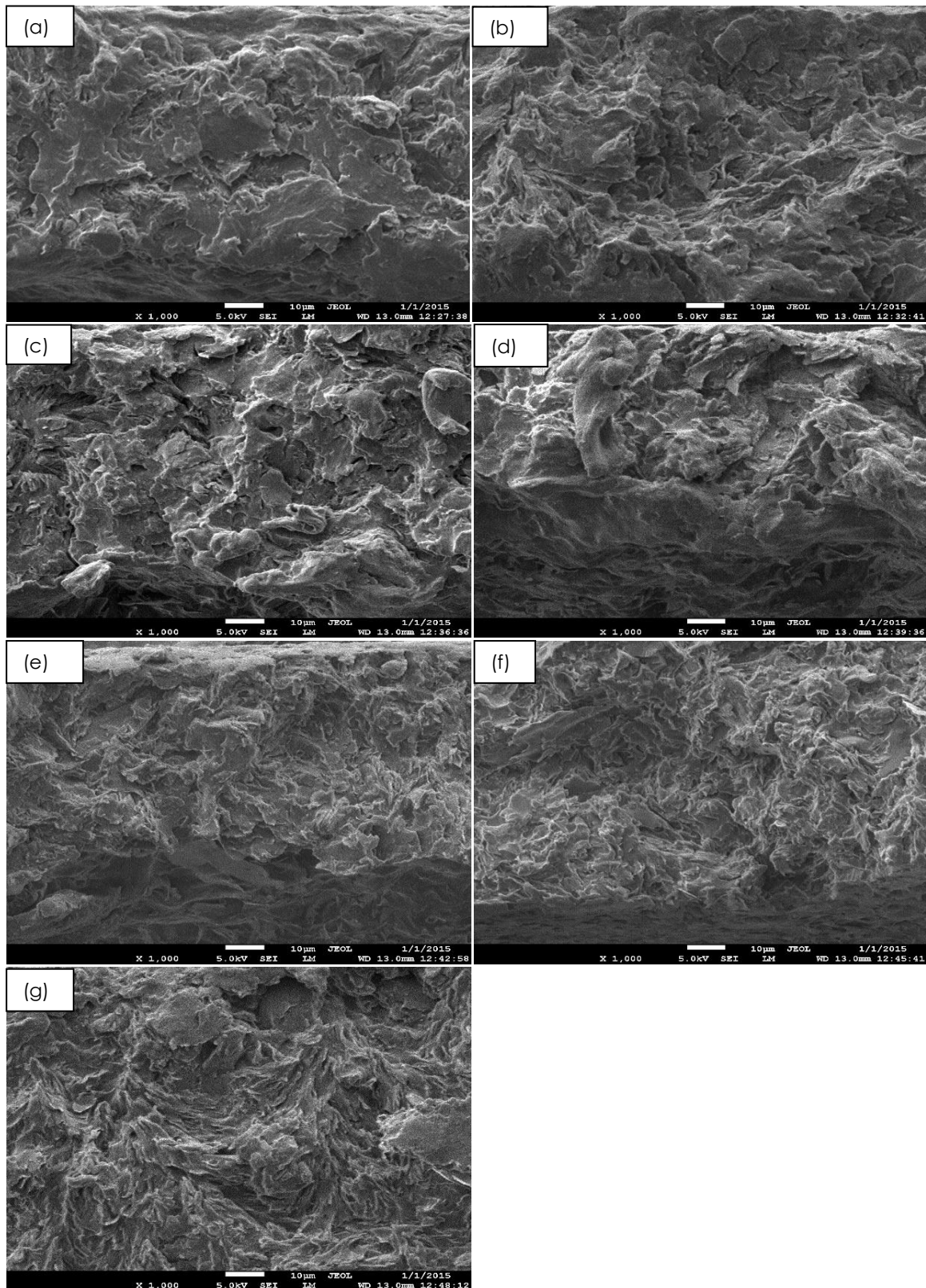


Figure 3 Chemical structure of graphite with/ within biopolymer matrix.



**Figure 4** FESEM cross-sectional images upon 1000x magnification of graphite/bio-based epoxy composites (a) neat, (b) 5 wt. %, (c) 10 wt. %, (d) 15 wt. %, (e) 20 wt. %, (f) 25 wt. %, (g) 30 wt. %.

### 3.3 Optical Properties

Figure 5 (a) shows the ultraviolet-visible spectra of graphite/ biopolymer composite with 5 wt%, 10 wt, 15 wt%, 20 wt%, 25 wt%, 30 wt% of graphite loading whilst Figure 5 (b) shows polypropylene-graphite composites [18] respectively.

The spectrum of each graphite/ biopolymer composite has an absorption peak in a range of 200

– 300 nm (graphene oxide has an absorption peak at 230 nm, 270 nm in graphene [19]). The absorption peak at 230 nm is referred to  $\pi$ - $\pi^*$  transition of aromatic C-C ring while on the other hand at 270 nm, is assigned to  $\pi$ - $\pi^*$  transition of C-O bonds now embedded using exfoliation and intercalation on the graphite. Both graphite- bioepoxy and graphite-polypropylene shows increasing absorption spectra vary to graphite weight loading.

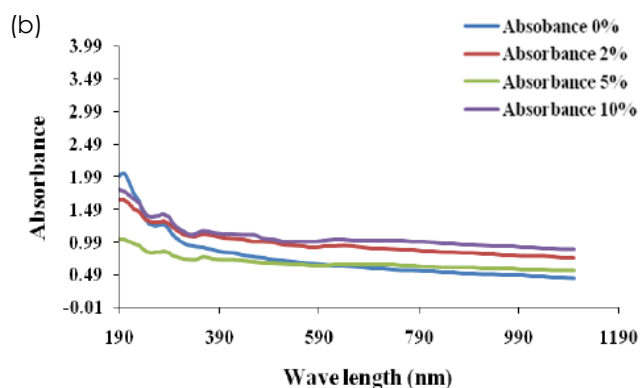
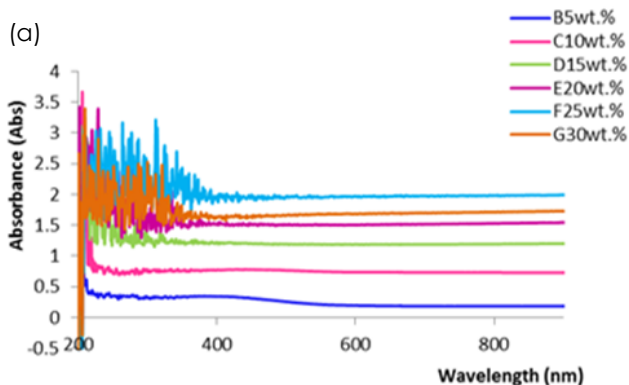


**Figure 5** UV-vis spectra of (a) graphite/ biopolymer composite, and (b) polypropylene-graphite composites [18] with varying graphite weight percentage loading (wt.%) as comparison

### 3.4 Functional Groups Characteristic

Figure 6 illustrates the FT-IR spectra of graphite/ biopolymer composites while varying the graphite weight loading (5, 10, 15, 20, 25 and 30 wt.%) with neat thin film as reference. There are no significant changes observed between those bands, exceptional for: higher shoulder at range  $3200\text{ cm}^{-1}$  and at  $2650.47\text{ cm}^{-1}$ , the decrease of polyether bands (C-O-C) at peak in a range  $1300\text{ cm}^{-1}$  –  $1100\text{ cm}^{-1}$ , and increasing aromatic bands (C=C) at peak range  $1600\text{ cm}^{-1}$  –  $1400\text{ cm}^{-1}$ . It should be noted that

the carbonyl group at peak  $1733.70\text{ cm}^{-1}$  is weaker hinting to the formation of (NHCOO) bond. The disappearance of the peak at around  $2260\text{ cm}^{-1}$ , assigned to the free isocyanate group, is sought to confirm that all the diisocyanate are consumed in the reaction.

Peak at  $3200\text{ cm}^{-1}$  is the stretching vibration absorption peak of the hydroxyl group in the structure of graphite/ biopolymer composites, which is from the water molecule. It might be due to the hygroscopicity of the original graphite, graphite oxide (GO), and pretreated graphite [20].

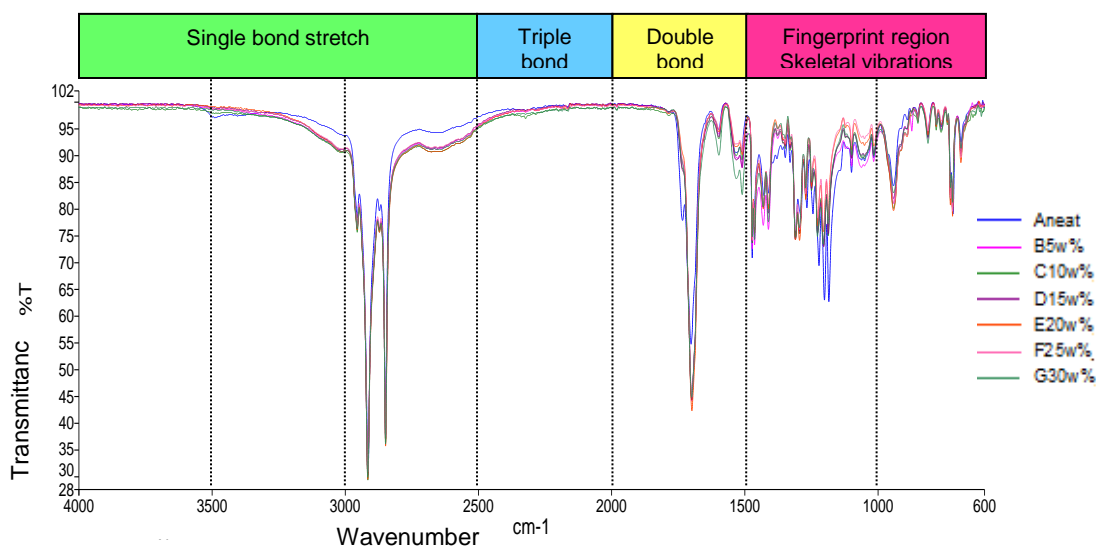


**Figure 6** FTIR spectrum of graphite/ biopolymer composites

### 3.5 Mechanical Behavior

Certain properties of samples such as tensile strength, elastic modulus and elongation at break are expected to be improved with addition of treated graphite in the biopolymer matrix. Figure 7 demonstrate the mechanical properties of composites with neat biopolymer thin film as reference, wherein increased of graphite weight loading respectively.

It can be clearly seen that the elastic modulus of the graphite/ biopolymer composites in Figure 7 (a) is increased than that of the neat biopolymer, which can be attributed to efficient load transfer between the treated graphite and the biopolymer matrix resulting from the chemical bonding and physical bonding. The study also revealed that as the elastic modulus increases, the tensile strength increases (Figure 7 (b)) with increases of graphite weight loading in the biopolymer matrix. Noted that both

modulus and strength of the thin film composites increased dramatically by about ~300% and ~200% respectively at the percolation threshold.

Figure 7 (c) indicates that the addition of pretreated graphite weight loading caused a decrease in elongation at break or break displacement of biopolymer composites. These mechanical behavior shows that the thin film composites having strong interfacial bonding between the pretreated graphite and matrix interfaces and aggregation of pretreated graphite in the biopolymer composites that increases the embrittlement and increases of graphite weight loading contribute to the stiffening effect. Hence, results proved that pretreated graphite have the synergistic effect on improving mechanical properties of biopolymer. A similar behaviour has also been observed for nanographite platelets (NGP) based polylactide (PLA) [21] and expanded graphite reinforced epoxy resin matrix [22].

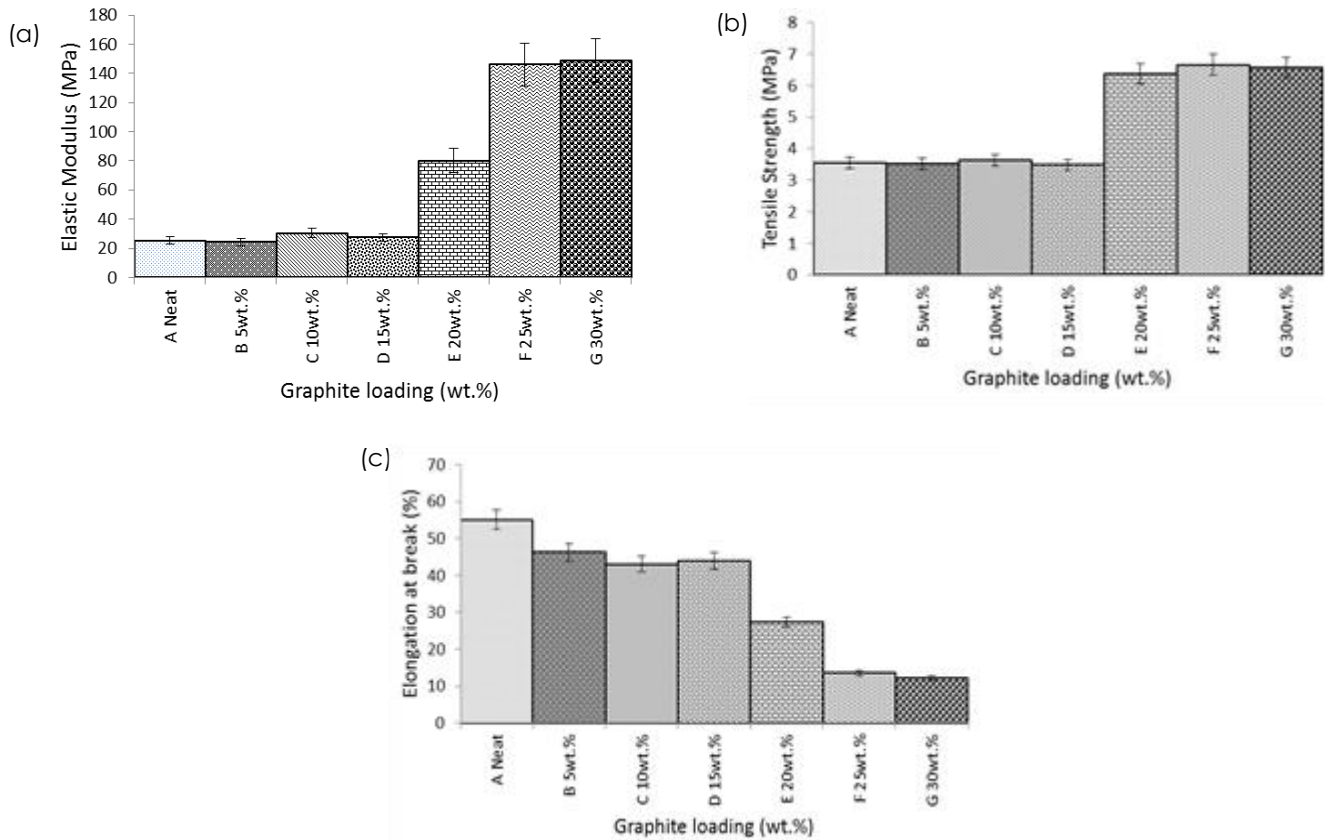


**Figure 7** The mechanical properties: (a) Elastic modulus (MPa), (b) Tensile strength and (c) Elongation at break (%) of graphite/biopolymer composites

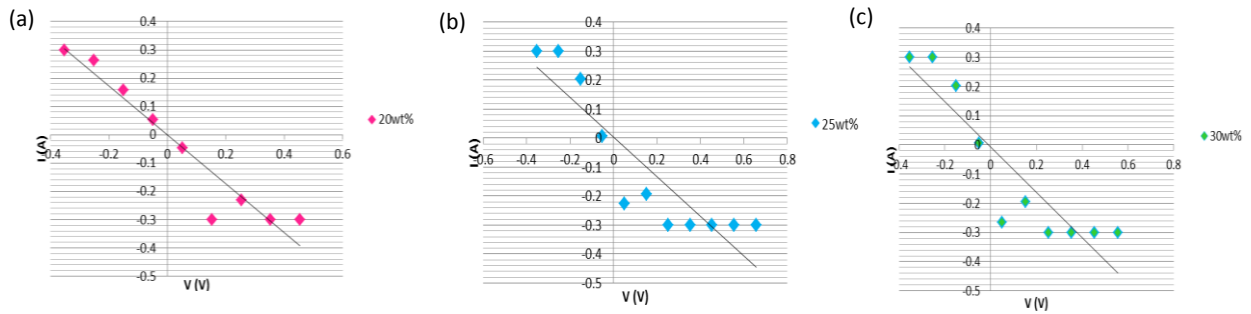


**Figure 8** I-V characteristic of graphite/ biopolymer composites at (a) 20 wt.%, (b) 25 wt.% and (c) 30 wt.% of graphite weight loading.

### 3.6 Electrical Measurement

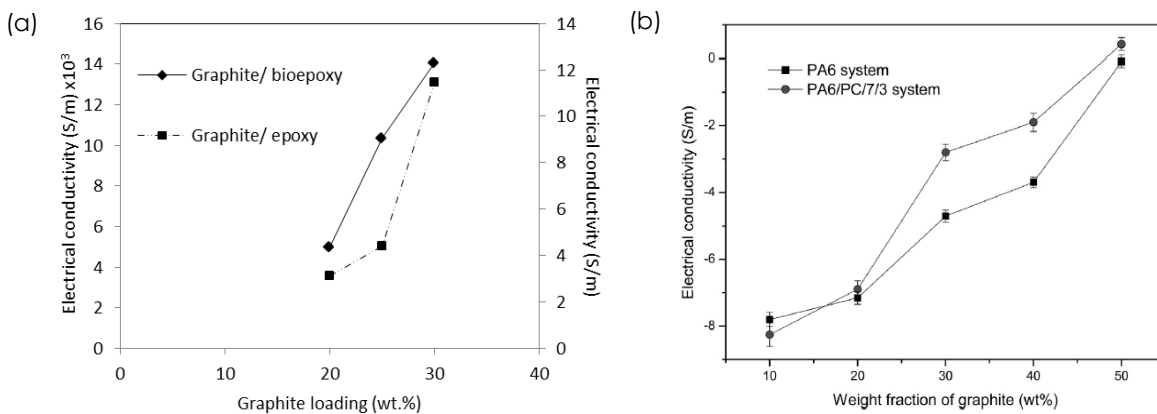
Figure 8 shows the I-V characteristic of 20 wt.%, 25 wt.%, 30 wt. % of graphite weight loading in the biopolymer composites. Meanwhile, low electron mobility in the composites might be the cause for lower graphite loading (5 wt. %, 10 wt. %, 15 wt. %) in both biopolymer and polymer composites having a low magnitude (lower than  $10^0$  S/m) of conductivity, where this characteristic cannot be justified by the graph.

Figure 9 (a) represents the electrical conductivity ( $\sigma$ ) values is plotted as a capacity of graphite weight loading (wt. %) in biopolymer and commercialized epoxy, and (b) graphite- polyamide 6/polycarbonate (PA6/PC) composites [23]. This figure shows that at the high weight loading of graphite in the polymeric materials concurrently amplifies electrical contacts between the particles and, as a result, the film resistivity decreases [24]. The graphs apparently shown that the calculated electrical conductivities from the reciprocal of the resistivity were increased by numerous orders of magnitude

from  $60-70 \times 10^3$  S/m upon 20 wt. %, 25 wt. %, and 30 wt.% of graphite/ biopolymer composites.

Noted that, the graphite/ epoxy composites achieved  $2-12 \times 10^0$  S/m upon 20 wt. %, 25 wt. %, and 30 wt.%. Meanwhile, graphite- PA6/PC composites achieved conductivity of  $10^{-7}-10^{-5}$  to 30- 40 S/m. Bare that slight differences in film thickness will jeopardize the film conductivity efficiency as thicker film will increase the resistivity.

As for lower graphite loading (5 wt. %, 10 wt. %, 15 wt. %), the graphite are covered by biopolymer chains where the composite does not form a conductive interconnected network in the insulating biopolymer matrix to reach the percolation limit. Sometimes, it is difficult to validate or invalidate the expected conduction mechanism by direct analytical measurements because of low currents implied. Hence, different measurement techniques should be occupied such as surface conductivity, DC conductivity, thermally stimulated DC current in understanding the relationship between their electrical properties [24].



**Figure 9** The electrical conductivity ( $\sigma$ ) of (a) graphite/ biopolymer and graphite/ epoxy, (b) graphite- polyamide 6/polycarbonate (PA6/PC) composites [23] as a function of graphite weight loading (wt.%).

## 4.0 CONCLUSION

Interaction between graphite- biopolymer implies a strong interfacial bonding, while functional properties of the composite greatly depend on the conductive structure of graphite. Notably, the values of the conductivity of the graphite/ biopolymer composite are  $60 - 70 \times 10^3$  S/m upon 20 wt.%, 25 wt.%, and 30 wt.% of graphite loading respectively. However, lower graphite loading at 5 wt.%, 10 wt.% and 15 wt.% in biopolymer composites need further discussed. As for the mechanical testing, the modulus and tensile strength of graphite/ biopolymer composites showed significant improvement with increased of treated graphite weight loading over its neat biopolymer counterpart, regardless the elongation at break of composites decreases as the functional group tends to decrease in composites with increasing filler content. Overall, the measured electrical properties gave a motivated considerable interest in the studies of graphite/ biopolymeric composite materials make now this field even more competitive.

## Acknowledgement

The authors would like to thank Universiti Tun Hussein Onn Malaysia (UTHM), Johor, and Malaysian Government for supporting this research under Fundamental Research Grant Scheme (Phase 1/2012), vot 1047. Extending the gratitude to Microelectronics and Nanotechnology – Shamsuddin Research Center (MiNT-SRC), UTHM and MyBrain15 scholarship.

## References

- [1] Hassan, N. N. M., Anika Zafiah, M. R. and Ghazali, M. I. 2014. Acoustic Performance of green polymer foam from renewable resources after UV exposure, *Int. J. Automotive and Mech. Eng.* 9: 1639-1648.
- [2] Anika Zafiah, M. R. 2009. Material properties of novelty polyurethane based on vegetable oils, The 11<sup>th</sup> International Conference on QIR (Quality in Research), Depok, Indonesia.
- [3] Siti Rahmah, M., Anika Zafiah M. Rus, and S.Nurulsaidatulsyida, 2013. Influence of N<sub>2</sub> and H<sub>2</sub>O on UV irradiated biopolymer composite, *International Conference on Mechanical Engineering Research (ICMER2013)*.
- [4] Zhang, S. M., Lin, L., Deng, H., Gao, X., Bilotti, E., Peijs, T., Zhang, Q. and Fu, Q. 2012. Synergistic effect in conductive networks constructed with carbon nanofillers in different dimensions. *eXPRESS Polymer Letters* .6(2): 159–168.
- [5] Shao, F. W., Shen, L., Wei, D. Z. and Yue, J. T. 2005. Preparation and mechanical properties of chitosan/carbon nanotubes composites. *Biomacromolecules*. 6: 3067- 3072
- [6] Yamamoto, N., Guzman deVilloria, R., Cebeci, H. G. and Wardle, B. L. 2010. Thermal and Electrical Transport in Hybrid Woven Composites Reinforced with Aligned Carbon Nanotubes. *Proceedings of the 51<sup>st</sup> AIAA/ASME/ASCE/AHS/ASC Structures, Structural Dynamics and Materials Conference*.
- [7] Siva Yellampalli (Ed.). 2011. Electrical Properties of CNT-Based Polymeric Matrix Nanocomposites, *Carbon Nanotubes – Polymer Nanocomposites*, InTech. ISBN: 978-953-307-498-6.
- [8] Sridhar, V., Lee, I., Chun, H. H., and Park, H. 2013. Graphene reinforced biodegradable poly(3hydroxybutyrate-co 4 hydroxybutyrate) nanocomposites. *eXPRESS Polymer Letters* .7(4):320–328.
- [9] Shih, W. P., Tsao, L. C., Lee, C. W., Cheng, M. Y., Chang, C. L., Yang, Y. J. and Fan, K. C. 2010. Flexible Temperature Sensor Array Based on a Graphite-Polydimethylsiloxane Composite. *Sensors*. 10: 3597-3610. ISSN 1424-8220.
- [10] Zhou, L. M., Feng, X., Mi, X. J., Li, Y. F., Xie, H. F. and Yin, X. Q. 2014. Mechanical reinforcement and shape memory effect of graphite nanoplatelet-reinforced epoxy composites. *Journal of Intelligent Material Systems and Structures*. 1-7.
- [11] Perween, M., Parmar, D. B., Bhadu, G. R. and Srivastava, D. N. 2014. Polymer-graphite composite: A versatile use & throw plastic chip electrode. *Analyst*. 139: 5919-5926.
- [12] Li, J. H., Li, J. and Li, M. 2007. Preparation of expandable graphite with ultrasound irradiation". *Materials Letters*. 61: 5070–5073.
- [13] Rus, A. Z. M. 2010. Polymers from renewable materials. *Science Progress*. 93 (3): 285-300.
- [14] Mohd Rus, A. Z., Kemp, T. J. and Clark, A. J. 2009. Degradation studies of polyurethanes based on vegetable oils. Part 2. Thermal degradation and materials properties. *Progress in Reaction Kinetics and Mechanism*. 34 (1): 1-41
- [15] Vadukumpully, S., Paul, J. Mahanta, N. and Valiyaveetil, S. 2011. Flexible Conductive Graphene/ Poly(vinyl Chloride) Composite Thin Films With High Mechanical Strength and Thermal Stability. *Carbon*. 49: 198-205.
- [16] Moazzami Gudarzi, M. and Sharif, F. 2012. Enhancement of Dispersion and Bonding of Graphene-Polymer Through Wet Transfer of Functionalized Graphene Oxide. *eXPRESS Polymer Letters*. 6(12): 1017-1031.
- [17] Murariu, M., Dechief, A. L. Bonnaud, L., Paint, Y., Gallos, A., Fontaine G. and Bourbigot, S. 2010. *Polym. Degrad. Stab.* 95.
- [18] Thema, F. T., Moloto, M. J., Dikio, E. D., Nyangiwe, N. N., Kotsedi, L., Maaza, M. and Khenfouch, M. 2013. Synthesis And Characterization of Graphene Thin Films by Chemical Reduction of Exfoliated and Intercalated Graphite Oxide. *Journal of Chemistry*. 6 .
- [19] Afroze, S., Rahman, M. M., Kabir, H., Kabir, Md. A., Ahmed, F. and Gafur, Md. A. 2012. Physical, optical and thermal properties of graphite and talk filler reinforced polypropylene (PP) composites. *Int. J. of Advanced Scientific and Technical Research*. 5(2). ISSN 2249-9954.
- [20] Liu, K., He, B. and Li, J. 2014. Conducting graphite/cellulose composite film as a candidate for chemical vapor-sensing material. *Peer-Reviewed Article In Bioresources*. 9(3): 5279- 5289.
- [21] Narimissa, E., Gupta, R. K., Choi, H. J., Kao, N. and Jollands, M. 2012. Morphological, mechanical, and thermal characterization of biopolymer composites based on polylactide and nanographite platelets. *POLYMER COMPOSITES*.
- [22] Yasmin, A., Luo, J. J., and Daniel, I. M. 2006. Processing of expanded graphite reinforced polymer nanocomposites. *Composites Science and Technology* 66 pp.1179–1186.
- [23] Roy, N., Sengupta, R. and Bhowmick, A. K. 2012. Modifications of carbon for polymer composites and nanocomposites, *Progress in Polymer Science* 37, pp. 781-819.
- [24] Bachari, T. S. 2014. Electric properties of Polyvinyl Acetate (PVA)- Polyol and prepared Sulfonated Phenol formaldehyde Resin (SPF) bulk samples composite. *Asian Journal of Applied Science and Engineering*. 3(2).ISSN 2305- 915X.